

Calorimetric and acoustic experiments on orientationally disordered and fully ordered crystalline phases of ethanol

This article has been downloaded from IOPscience. Please scroll down to see the full text article.

2007 J. Phys.: Condens. Matter 19 205135

(<http://iopscience.iop.org/0953-8984/19/20/205135>)

View [the table of contents for this issue](#), or go to the [journal homepage](#) for more

Download details:

IP Address: 129.252.86.83

The article was downloaded on 28/05/2010 at 18:49

Please note that [terms and conditions apply](#).

Calorimetric and acoustic experiments on orientationally disordered and fully ordered crystalline phases of ethanol

M A Ramos¹, V Rodríguez-Mora¹ and R J Jiménez-Riobóo²

¹ Laboratorio de Bajas Temperaturas, Departamento de Física de la Materia Condensada, C-III, Universidad Autónoma de Madrid, Cantoblanco, 28049 Madrid, Spain

² Instituto de Ciencia de Materiales de Madrid, CSIC, Cantoblanco, 28049 Madrid, Spain

E-mail: miguel.ramos@uam.es

Received 11 October 2006

Published 25 April 2007

Online at stacks.iop.org/JPhysCM/19/205135

Abstract

Ethanol exhibits a very interesting polymorphism, presenting different solid phases below its melting point at 159 K: a structural (amorphous) glass, by quenching the supercooled liquid below the glass-transition temperature $T_g = 97$ K; a (bcc) plastic crystal, which by quenching below the same $T_g = 97$ K becomes an orientationally disordered crystal with glassy properties (sometimes named a '*glassy crystal*'); and fully ordered (monoclinic) crystals. We present here new calorimetric experiments and specific-heat measurements of the different phases of ethanol in the relevant temperature range around the glass-transition and melting temperatures. In addition, we have concurrently performed Brillouin-scattering experiments on these crystalline phases, both fully ordered and orientationally disordered ones, that complement our earlier studies of the glass phases. The possible role of water impurities in kinetic and thermodynamic properties has also been investigated.

(Some figures in this article are in colour only in the electronic version)

1. Introduction

Ethanol ($\text{CH}_3\text{CH}_2\text{OH}$) is a very well known chemical substance, widely used in daily life, which has even been used as a glassy matrix in experimental work. Also, ethanol is one of the six glass-formers which appeared in the famous paper by Kauzmann [1]. It is known [2–7] that ethanol is polymorphic, presenting different solid phases: a fully ordered (monoclinic) crystal, a (bcc) plastic crystal (PC), which by quenching becomes an orientationally disordered crystal (ODC) with glassy properties (hence sometimes named a '*glassy crystal*' or even orientational glass), and the ordinary, amorphous glass. Indeed, the ODC of ethanol exhibits [4–7] the

same universal behaviour in low-temperature properties and low-frequency dynamics as the conventional glass, hence the alternative use of the names *glassy crystal* or *orientational glass*.

It may be pointed out that the ‘glass transition’ of ethanol presented by Kauzmann in 1948—using the earlier, available data of Parks, Kelley and others [8]—did not correspond to the true, standard liquid–glass transition but rather to a dynamical transition from the PC phase of ethanol (i.e. a crystal with *rotational* disorder) into the ODC phase (a crystal with static, *orientational* disorder). As first found by Haida *et al* [2], the canonical (amorphous) glass of ethanol was only obtained from the liquid by a much faster cooling rate (around -30 K min^{-1}). Very interestingly, both the standard glass transition and the dynamical freezing of the PC into the ODC were found to occur at the same temperature ($T_g \approx 97 \text{ K}$) and with comparable discontinuities in the specific heat.

Furthermore, we have recently [9] found that there exist at least four different monoclinic crystalline phases of ethanol, in addition to the cubic glassy crystal and the truly amorphous glass.

In this paper we present new calorimetric and acoustic experiments performed between 80 and 180 K, hence in the temperature range where all the relevant phase transitions take place, and compare them with previous experimental data when available. We have employed different qualities of ethanol purity in order to study the possible influence of water content on the physical properties measured on ethanol, as well as on crystallization and vitrification kinetics.

2. Experimental details

2.1. Calorimetry

Calorimetric experiments were performed using the same experimental set-up developed earlier and used to measure the specific heat of ethanol at low temperatures [4–7]. A silicon diode was used as the thermometer in the whole temperature range, and a $1 \text{ k}\Omega$ resistor as the electrical heater. The temperature of the internal vacuum chamber was controlled automatically. Small copper cells were employed (typically with 3.3 g of addenda and 2 cm^3 of liquid volume, with a thin copper mesh fitted inside to facilitate thermal equilibrium). The heat capacity of one empty cell was measured independently and under the very same conditions in order to subtract its contribution. Small differences in weight (less than 5%) among different cells were taken into account by considering the specific heat of copper. Experiments were run in a glass cryostat, using nitrogen as the cryogenic liquid, and were conducted in a high-vacuum environment ($\leq 10^{-7} \text{ mbar}$).

Since the measurements were made in a sealed calorimeter under their own vapour pressure, the obtained data are, strictly speaking, heat capacities at saturation pressure C_s . However, their differences from the usual heat capacities at constant pressure C_p are negligible, and the latter term will be used hereafter. Specific-heat data presented in this work were obtained by employing a quasi-adiabatic, continuous method. The calorimetric cell is in contact with the thermal reservoir at 77 K through an effective thermal link (mainly arising from blackbody thermal radiation plus conduction through the electrical wiring). Therefore, the equation of heat transport contains both cooling P_{cool} and a heating P_{heat} power terms, so that

$$C_p \left(\frac{dT}{dt} \right) = P_{\text{heat}} + P_{\text{cool}} = V_h I_h + C_p \tau(T) \quad (1)$$

where V_h and I_h are the voltage applied to the heater element and the electric current flowing through it, respectively, and $\tau(T) \equiv dT/dt$ is the intrinsic (negative) thermal drift of the

system, which is directly measured as a function of temperature by standard cooling at $I_h = 0$, with the thermal reservoir fixed at 77 K. Therefore, the heat capacity of the cell can be determined from:

$$C_p = \frac{V_h I_h}{\left(\frac{dT}{dt} - \tau(T)\right)}. \quad (2)$$

On the other hand, a direct display of the measured dT/dt curve as a function of temperature T , for a constant applied power, is a useful method to investigate first-order transitions such as melting and crystallization processes.

2.2. Brillouin scattering

High-resolution Brillouin spectroscopy (HRBS) spectra were recorded using a Sandercock 3 + 3 Tandem spectrometer. The light source was an Ar⁺ laser, and in order to change the temperature an Oxford Instruments continuous flow cryostat (Optistat) was used. Temperature stabilization was achieved with an ITC-4 controller (Oxford Instruments). The ethanol samples were contained in rectangular optic cuvettes (Starna) with optical paths of 0.5 or 1 mm. The backscattering geometry (180°) was used in these experiments, which implies a refractive-index dependent acoustic wavevector. The corresponding wavevector is:

$$q^{180} = \frac{4\pi n_i}{\lambda_0}. \quad (3)$$

λ_0 stands for the laser wavelength and n_i for the refractive index of the sample. The sound propagation velocity (v) results from the combination of the Brillouin frequency shift, f , and the corresponding acoustic wavevector:

$$v^{180} = \frac{f^{180} \lambda_0}{2n_i}. \quad (4)$$

2.3. Materials

In the present work we have employed ‘dry’ ethanol (nominal maximum H₂O content 0.02%), pro-analysis ethanol (nominal maximum H₂O content 0.1%) and commercial ethanol (96% v/v pure) to study the possible influence of water content on the thermodynamic and kinetic properties of ethanol. We did not do any further purification and the real amount of water impurity in ethanol samples was confirmed by measuring the index of refraction at 20 °C and comparing it with literature values [10].

3. Results and discussion

3.1. Different crystalline phases

Ethanol is a unique case, since it is feasible to obtain it in several different solid phases [2–7] depending on the thermal history: as fully ordered (monoclinic) crystal; as conventional (amorphous) glass below $T_g \approx 97$ K by quenching the supercooled liquid faster than -30 K min⁻¹ [2]; as a (bcc [3]) plastic crystal by cooling the liquid at an intermediate rate (a few K min⁻¹); as an ODC or *glassy crystal* [2] obtained by quenching this plastic crystal also below $T_g \approx 97$ K. Indeed, the exact critical cooling rates required to obtain the glassy phases depend appreciably on the experimental cell, as discussed in [9].

By a concurrent use of x-ray diffraction and calorimetric techniques, we have recently found [9] that there exist at least four different (all monoclinic) crystalline varieties or phases of

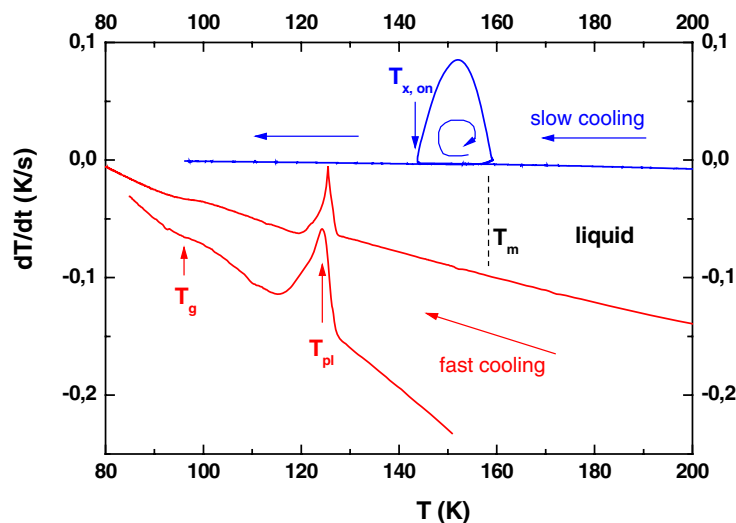


Figure 1. Directly measured variations of temperature as a function of time, when cooling liquid ethanol at different rates. Slow cooling (upper curve) below the melting temperature $T_m = 159$ K led to the stable crystal, with an onset of crystallization (self-heating loop) observed around $T_{x,on} = 143$ K. Faster cooling rates (lower curves) produced the plastic crystal (exothermic peaks) at $T_{pl} \approx 125$ K.

ethanol, in addition to the above mentioned cubic glassy crystal and the truly amorphous glass. Although the monoclinic crystalline phase has usually [2–7] been obtained by heating the PC phase above 120 K (let us call it α crystal [9]), it is also possible to obtain it by slow cooling of the supercooled liquid (SCL). As shown in figure 1 (upper curve), when cooling the liquid at a rate around -0.2 K min^{-1} , a strong exothermic process, characteristic of a crystallization, is observed to start at $T_{x,on} = 143$ K in our case. After the self-heating effect produced (the loop seen in the curve), the crystal continues its cooling process. We designated [9] the so-obtained crystal as γ -crystal, and our above mentioned x-ray diffraction experiments confirmed that it corresponded to a monoclinic phase.

We also have shown [9] that these crystalline phases exhibit (slight) differences in their structures and thermal behaviour. The usually obtained (α) phase (see figure 2) is metastable and undergoes an exothermic process around 145 K into another (β) phase. On the other hand, the (γ) crystalline phase obtained by slowly cooling the liquid below its melting temperature $T_m = 159$ K is the stable phase at low temperatures. It also exhibits a small endothermic process (see figure 2) around 150 K into another (δ) phase. These two features are indicated by arrows in figures 2 and 4 (see more details and data in [9]). These higher temperature crystalline phases, β and δ , were resolved as different phases by diffraction experiments [9], though we were not able to resolve them by calorimetry. Nevertheless, the specific heats of both low-temperature monoclinic phases, α and γ , are the same within experimental error in the studied temperature range (see figures 3 and 4), and are also in good agreement with previous data in the literature [2]. In figure 5, HRBS experiments confirm the liquid \rightarrow γ -crystal transition around $T_x = 145$ K and the slight crystalline modifications when heating the γ -crystal, before melting.

On the other hand, when the liquid is cooled at a faster rate (typically between -1 and -20 K min^{-1} , see examples in figure 1), the γ -crystallization is bypassed, and the SCL enters the PC phase at $T_{pl} \approx 125$ K, as evidenced by the exothermic peaks, and eventually the orientationally disordered *glassy* crystalline phase below 97 K.

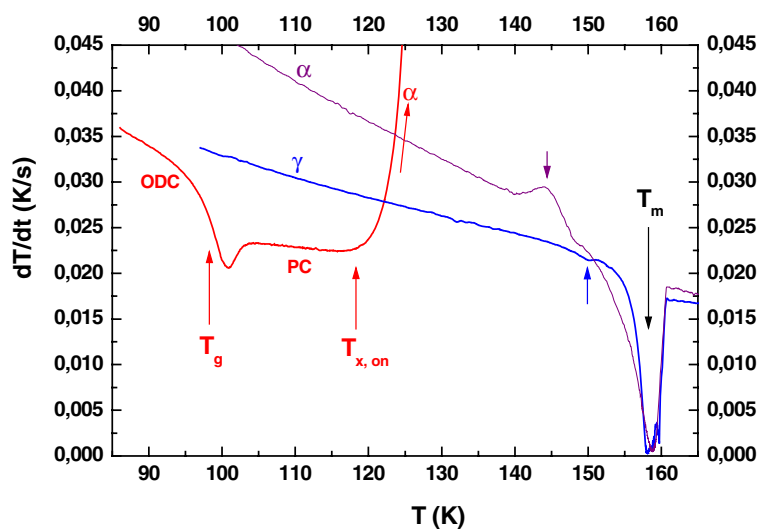


Figure 2. Directly measured variations of temperature as a function of time, at different constant heating powers, for different phases of ethanol. Lower curve: the ODC experiences the ‘glass transition’ into the PC phase and crystallization into the α phase. Upper curve: the previously obtained α -crystal is heated up to melting, exhibiting a small exothermic peak at 145 K. Mid curve: heating of the γ -crystal up to melting, exhibiting a small endothermic peak around 150 K.

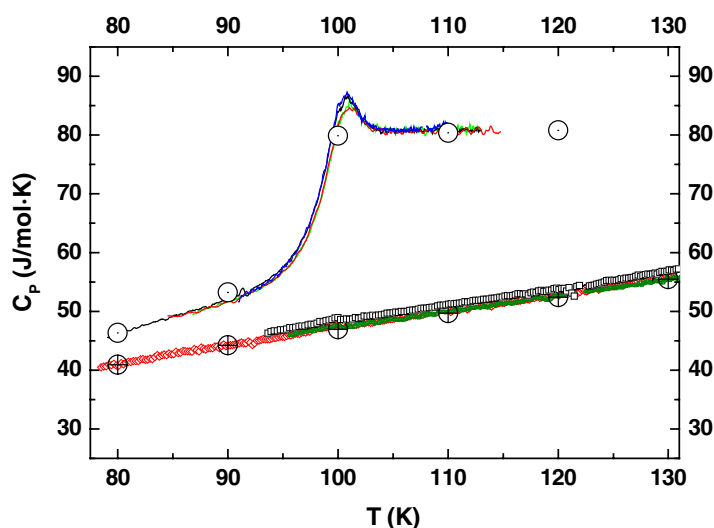


Figure 3. Molar specific heat of ODC-PC phases (upper curves) and mono-clinic crystalline α and γ phases of ethanol. Five different (almost indistinguishable) upper solid curves correspond to different experimental runs. Four different (almost indistinguishable) symbols below correspond to two α -crystals and to two γ -crystals. Dotted circles (ODC-PC) and crossed circles (crystal) are data from Haida *et al* [2].

3.2. Dynamic glass transition PC \leftrightarrow ODC

When the above mentioned ODC phase is heated and measured, a dynamic ‘glass transition’ (the release of the orientational degrees of freedom, frozen-in for the ODC) is observed at

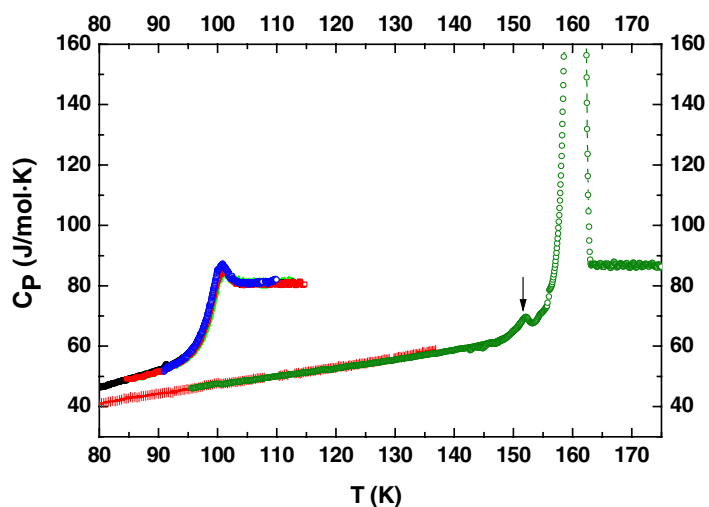


Figure 4. Molar specific heat of ODC-PC phases (five indistinguishable upper curves) and monoclinic crystalline phases α (crosses) and γ (circles) of ethanol. The arrow at 152 K features the endothermic process assigned to the $\gamma \rightarrow \delta$ transition. Melting is observed at $T_m = 159$ K.

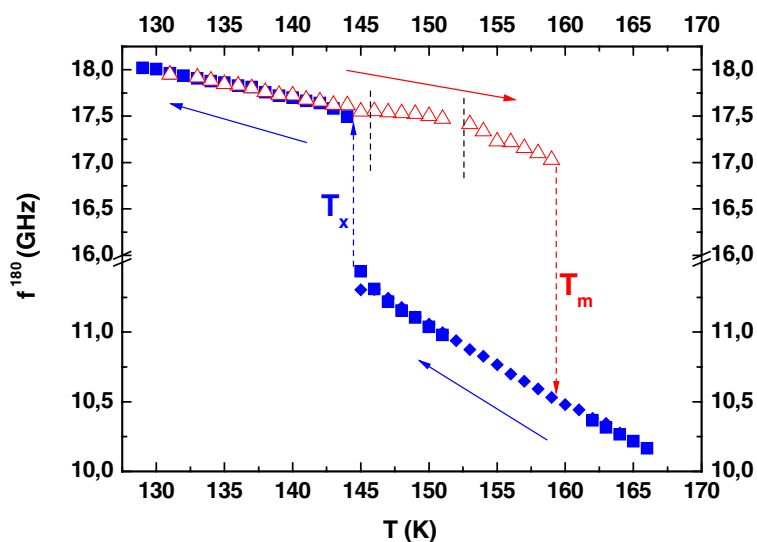


Figure 5. Backscattering Brillouin frequency shift measured during a slow-cooling curve (solid symbols) of pure ethanol below its melting temperature $T_m = 159$ K until γ -crystallization occurs at $T_x \approx 145$ K. The heating curve (open symbols) of this γ -crystal is also shown. The dashed bars indicate a temperature region where possible crystal-crystal transitions are taking place.

$T_g \approx 97$ K, above which the substance becomes a plastic crystal. Experimental evidence of this transition is the endothermic feature in figure 2 and the corresponding specific-heat data in figures 3 and 4. After further heating above 120 K, the PC irreversibly transforms, via a first-order transition, into a fully ordered (α) crystal (see the lower curve in figure 2).

The same SCL \rightarrow PC and PC \rightarrow ODC transitions have been observed in our Brillouin-scattering experiments, as shown in figure 6, where the liquid was cooled down to 130 K and

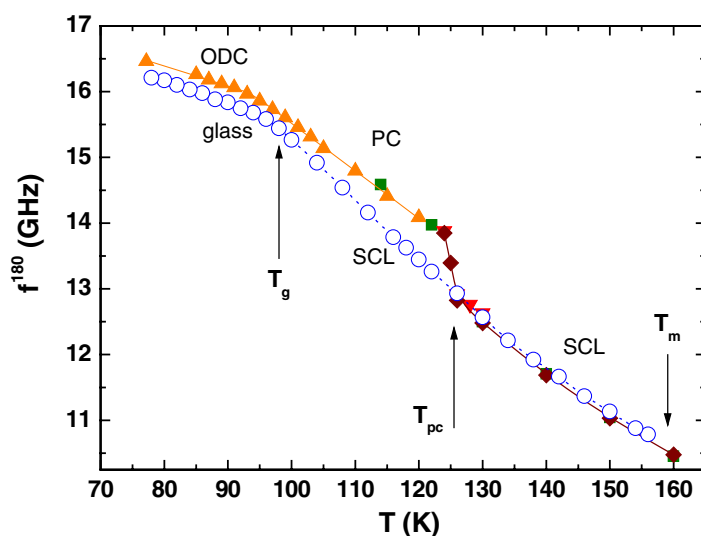


Figure 6. Data obtained in different cooling runs with backscattering geometry for ‘dry’ samples of ethanol. Different solid symbols correspond to different cooling runs. Below 130 K the cooling rate used was always very slow ($-0.033 \text{ K min}^{-1}$). T_{pc} stands for the transition from supercooled liquid to plastic crystal, and T_g for the glass-transition temperatures (either conventional or orientational). Open circles correspond to data obtained with ethanol having $0.24 \pm 0.25\%$ of water impurity, by cooling at -0.06 K min^{-1} which bypassed the plastic crystallization. Lines are only guides for the eye.

then further cooled very slowly ($-0.033 \text{ K min}^{-1}$). As can be seen, around $T_{pl} \approx 125 \text{ K}$ a sudden increase in the sound-velocity signal features the SCL \rightarrow PC transition.

Our claim that this dynamical transition ODC \rightarrow PC can be considered a proper glass transition (in addition to the observed similarities between it and the canonical one, as mentioned above) is supported by the experiments shown in figure 7. There, specific-heat curves for pure ethanol ($<0.1\%$ water) across the dynamic glass-transition ODC \rightarrow PC are shown for *glassy crystals* which have been subjected to two different kinds of thermal history during their preparation. The ODC of the upper curve of figure 7 was obtained by slow cooling (about -0.05 K min^{-1}) and exhibits a very pronounced peak (overshoot) at T_g compared to other samples quenched between -2 and -6 K min^{-1} . Therefore, the former ODC was cooled more slowly than the heating rate employed during the calorimetric measurement (approximately $+1.2 \text{ K min}^{-1}$), whereas the latter samples were on the contrary obtained at a faster cooling rate than heating rate. The observed behaviour is typically found in the glass transition of conventional glasses and attributed to the special distribution of relaxation times characteristic of the glassy state.

In figure 7, we also present the method that we have used to determine the glass-transition temperatures and specific-heat discontinuities: for the ODC \rightarrow PC transition of pure ethanol (both dry and pro-analysis), we obtain $T_g = 98 \text{ K}$ and $\Delta C_p(T_g) = 24.0 \text{ J mol}^{-1} \text{ K}^{-1}$, in good agreement with previously published data [2].

3.3. Effect of water impurities

In previous experiments [9] we emphasized the relevance of the experimental cell (the shape and peculiarities of the container where the liquid ethanol is cooled) for the crystallization

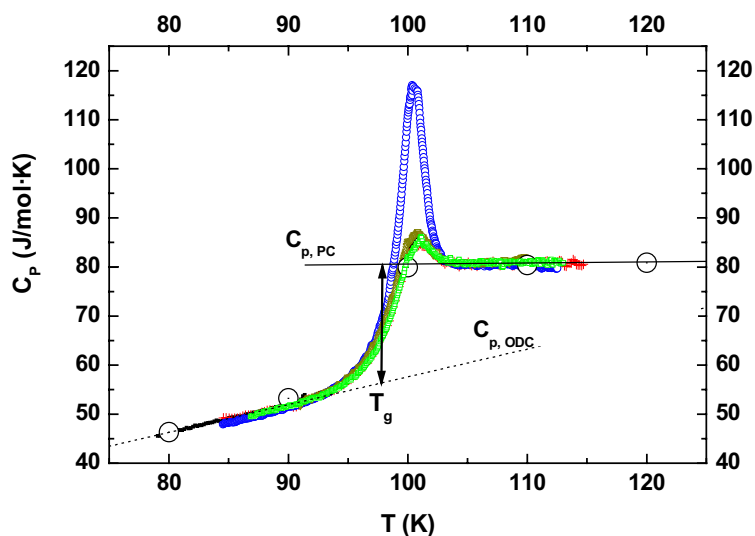


Figure 7. Temperature dependence of the specific heat of pure ethanol (<0.1% water) across the dynamic glass-transition ODC \rightarrow PC region for two different kinds of thermal history: The upper curve (small circles), obtained by slow cooling (about -0.05 K min^{-1}), exhibits a more pronounced peak (overshoot) at T_g compared to the samples quenched between -2 and -6 K min^{-1} (lower symbols). These heat-capacity measurements were performed using the continuous method at a heating rate of approximately $+1.2 \text{ K min}^{-1}$. The method to determine $T_g = 98 \text{ K}$ and $\Delta C_p(T_g) = 24.0 \text{ J mol}^{-1} \text{ K}^{-1}$, as the midpoint of the discontinuity, is graphically indicated. Dotted circles are data from Haida *et al* [2] for their ‘glassy crystal’.

kinetics and glass-forming ability. Later [11] we also studied the influence of small amounts of water, finding that H_2O fractions in ethanol as low as 0.2–0.7% are enough to hinder the plastic crystallization when cooling the SCL in some cases and permit the SCL to transform into the glass at very slow cooling rates.

Therefore, in order to determine the amount of water present in the ethanol used and assess its possible influence on the results, we have measured the index of refraction of the sample before and after the experiment. For this purpose, an optical Abbe refractometer (Krüss) was used. The index of refraction n_D^{20} of the monochromatic D line of the sodium spectrum at 20°C can be compared with published data [10] for the binary ethanol–water mixture, and interpolated for the lowest water concentrations. For the corrections when measuring at temperatures of not exactly 20°C , the linear rate $dn_i/dT = -(4.29 \pm 0.02) \times 10^{-4} \text{ K}^{-1}$ found in [12] was considered. We estimate an absolute error of $\pm 0.25\%$ in the derived H_2O content, though the relative comparison among different cases is surely better. In all the cases shown up to now, employing either dry or pro-analysis ethanol, the amount of water measured *after* the calorimetric experiments was always below $0.19 \pm 0.25\%$.

Moreover, we have conducted similar calorimetric experiments on commercial ethanol (96% v/v pure), for which we determined a water content of $3.4 \pm 0.4\%$. Figures 8 and 9 show the specific-heat curves that we have obtained for the glass phase (produced by just slowly supercooling the liquid) and for the stable crystal phases (only observed when heating the SCL from lower temperatures). The PC and ODC phases seem not to already exist with this amount of water. The absolute values of the specific heat of both glass and crystal are very similar to those of pure ethanol (see figure 8). The glass transition and melting temperatures are different however: $T_g = 102 \text{ K}$ (4 K higher than pure ethanol) and $T_m = 151 \text{ K}$ (8 K

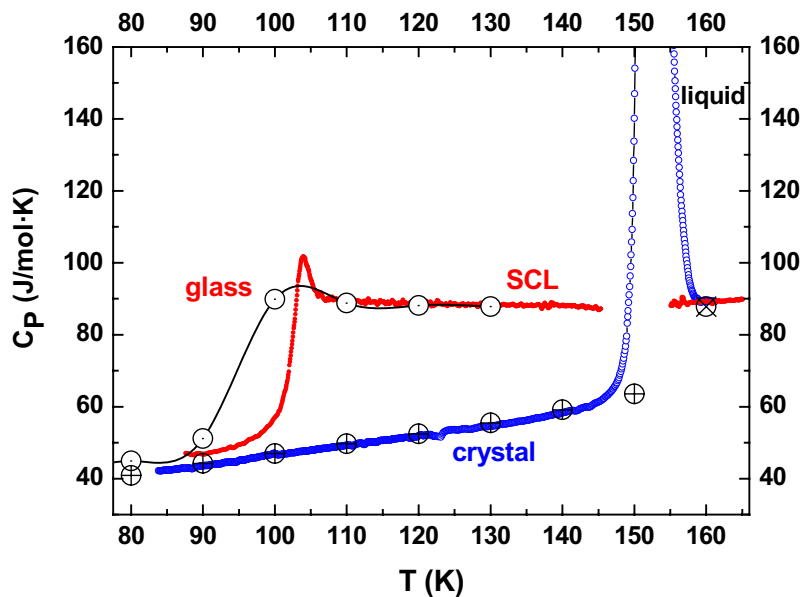


Figure 8. Molar specific heat of the different phases (crystal, glass and liquid) of commercial ethanol (96% v/v pure). The melting is observed to occur at $T_m = 151$ K. Dotted circles (glass-supercooled liquid) and crossed circles (crystal) are data from Haida *et al* [2].

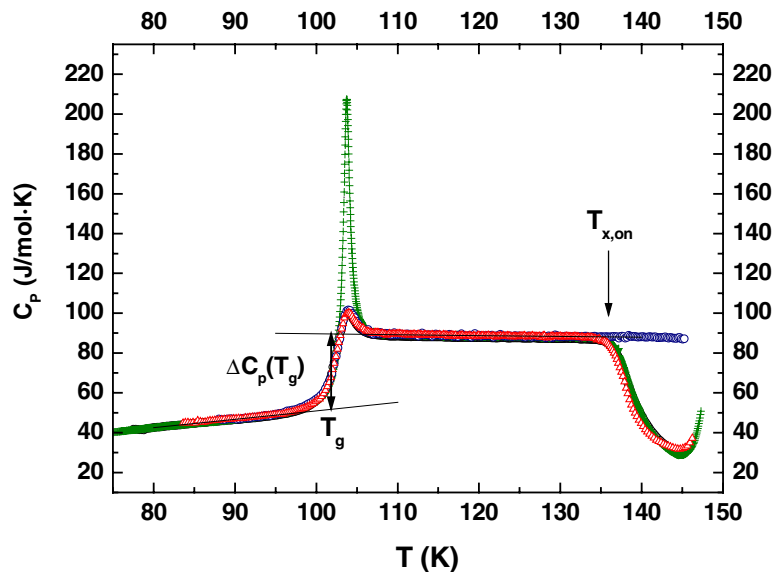


Figure 9. Temperature dependence of the specific heat of commercial ethanol (96% v/v pure) across the canonical glass-transition region for two different kinds of thermal history: The upper curve (crosses), obtained by slow cooling (about -0.05 K min^{-1}), exhibits a much more pronounced peak (overshoot) at T_g compared to the samples quenched between -3 and -5 K min^{-1} (lower symbols). These heat-capacity measurements were performed consecutively using the continuous method at a heating rate of approximately $+1.2$ K min^{-1} . The method to determine $T_g = 102$ K and $\Delta C_p(T_g) = 37.7$ J mol^{-1} K^{-1} , as the midpoint of the discontinuity, is graphically indicated. Above $T_{x,on} = 137$ K, the SCL crystallizes, unless one employs a faster heating rate (circles).

lower than pure ethanol). The latter could be due to a eutectic point presumably located at low water concentrations, and the former to a mixture effect produced by the higher T_g of water. As a combined result, the temperature window between T_g and T_m is reduced significantly, accounting for the much better glass-forming ability of commercial ethanol.

4. Summary and conclusions

We have presented new calorimetric experiments and specific-heat measurements of the different phases of ethanol between 80 and 180 K, hence in the relevant temperature range around the glass transitions and crystallization/melting processes, as well as Brillouin-scattering experiments, with special focus on the different crystalline phases of ethanol, either fully ordered or orientationally disordered ones. Our results provide further support for previous experimental findings. We have also shown that the dynamic ODC \rightarrow PC transition behaves calorimetrically as any standard glass transition in all respects, showing that the glass transition phenomenon is a more general one than just the dynamic arrest of a fluid into an amorphous solid.

The possible role of water impurities in kinetic and thermodynamic properties has also been investigated. For water contents below, say, 1%, glass-forming ability coexists with the ODC and PC phases and several varieties of the monoclinic, fully ordered crystal. Very interestingly, commercial ethanol (around 3.5% water) appears to be an excellent glass-former, though it does not seem to exhibit the plastic crystal phase nor more than one stable crystal. The melting temperature of ethanol *decreases* with increasing water content at low concentrations, probably due to the existence of some eutectic point at those low water concentrations, whereas the glass transition *increases*. Therefore, we plan to investigate the thermodynamic behaviour of ethanol–water mixtures for relatively small water concentrations.

Acknowledgment

This work was supported by the Spanish Ministry of Education and Science within project BFM2003-04622.

References

- [1] Kauzmann W 1948 *Chem. Rev.* **43** 219
- [2] Haida O, Suga H and Seki S 1977 *J. Chem. Thermodyn.* **9** 1133
- [3] Srinivasan A, Bermejo F J, de Andrés A, Dawidowski J, Zúñiga J and Criado A 1996 *Phys. Rev. B* **53** 8172
- [4] Ramos M A, Vieira S, Bermejo F J, Dawidowski J, Fisher H E, Schober H, González M A, Loong C K and Price D L 1997 *Phys. Rev. Lett.* **78** 82
- [5] Talón C, Ramos M A, Vieira S, Cuello G J, Bermejo F J, Criado A, Senent M L, Bennington S M, Fischer H E and Schober H 1998 *Phys. Rev. B* **58** 745
- [6] Talón C, Ramos M A and Vieira S 2002 *Phys. Rev. B* **66** 012201
- [7] Ramos M A, Talón C, Jiménez-Riobóo R J and Vieira S 2003 *J. Phys.: Condens. Matter* **15** S1007
- [8] Gibson G E, Parks G S and Latimer W M 1920 *J. Am. Chem. Soc.* **42** 1542
Parks G S 1925 *J. Am. Chem. Soc.* **47** 338
Kelley K K 1929 *J. Am. Chem. Soc.* **51** 779
- [9] Ramos M A, Shmyt'ko I M, Arnautova E A, Jiménez-Riobóo R J, Rodríguez-Mora V, Vieira S and Capitán M J 2006 *J. Non-Cryst. Solids* **352** 4769
- [10] Lide D R (ed) 2005 *Handbook of Chemistry and Physics* (Boca Raton, FL: CRC Press) chapter 8, p 63
- [11] Jiménez-Riobóo R J and Ramos M A 2006 *Phil. Mag.* at press
- [12] Fan C H 1998 Laser-based measurements of liquid refractive index, concentration and temperature *PhD Thesis* Stony Brook, NY